Low-Cost Recuperative Heat Exchanger for Supercritical Carbon Dioxide Power Systems

Final Scientific/Technical Report

For

Reporting Period Starting October 1, 2014 Ending June 30, 2019

By

Dr. John T. Kelly

Issued October 31, 2019

DOE Award No. DE-FE 0024058

Submitted by:
Altex Technologies
244 Sobrante Way
Sunnyvale, CA 95070
john@altextech.com
408-328-8302

DISCLAIMER

This report was prepared as an account of work sponsored by an agency of the United States Government. Neither the United States Government nor any agency thereof, nor any of their employees, makes any warranty, express or implied, or assumes any legal liability or responsibility for the accuracy, completeness, or usefulness of any information, apparatus, product, or process disclosed, or represents that its use would not infringe privately-owned rights. Reference herein to any specific commercial product, process, or service by trade name, trademark, manufacturer, or otherwise does not necessarily constitute or imply its endorsement, recommendation, or favoring by the United States Government or any agency thereof. The views and opinions of authors expressed herein do not necessarily state or reflect those of the United States Government or any agency thereof.

ABSTRACT

Closed Brayton super-critical CO_2 power cycles are well suited to waste heat bottoming cycles, due to their increased efficiency and compactness, relative to Rankine steam bottoming cycles. Since waste heat applications would be retrofits, the power system compactness is important. To achieve high efficiency, these power cycles require high pressure recuperative type heat exchangers, of substantial heat duty. Current Printed Circuit Heat Exchangers (PCHE), originally developed for high pressure gas and oil applications, can be used as recuperators, but costs are higher than desired. Altex is developing a purpose-built high pressure and effectiveness recuperator to provide the reliability, compactness, performance and pressure capability of current recuperators, but at a reduced cost. The High Effectiveness Low Cost (HELC) recuperative heat exchanger design yields volume and weight metrics of .0024 m^3/UA and 10.2 kg/UA, which are 4% and 77.3% below recuperator target metrics, respectively. A 50 kW test article was designed and fabricated. Performance tests on water and oil showed that the HELC design model could predict heat transfer, to within 10% of the measured value. This model was then used to project HELC performance, when operating on supercritical CO_2. Besides performance tests, the test article was hydrostatically tested, for integrity at up to 4,000 psi pressure. At these conditions, some distortion of channels was encountered. To mitigate distortion, the inserts were redesigned and these results were used to project the cost of 500 kW and 5,083 kW HELC units. The cost metric for the 5,083 kW unit was determined to be $1,349/UA, which is 10% lower than the recuperator desired cost metric desired target of $1,500/UA. In addition, the 5,083 kW unit HELC cost of $61.09/kW is 33.6% lower than the $92/kW estimated cost for a PCHE. Hydrostatic pressure tests, at up to 4,000psi, showed that the unit did not leak. However, channels were distorted at this pressure differential. Design updates to minimize stress concentrations and distortion were prepared and analyzed, to show that distortion could be controlled, but to date tests have not been run to prove the design. Project results show the potential of the HELC approach, but more work is required to confirm this potential, at the larger scales of interest.

TABLE OF CONTENTS

ABSTRACT 3

EXECUTIVE SUMMARY 5

1.0 Introduction 7

2.0 Application, Goals and Specifications 8

3.0 Full-Scale and Test Article Designs 10

4.0 Heat Transfer Enhancement 16

5.0 Test Articles and Performance and Integrity Testing 18

6.0 Cost Estimates 27

7.0 Conclusions 30

References 31

EXECUTIVE SUMMARY

Recompression Closed Brayton super-critical CO_2 power cycles are well suited to waste heat bottoming cycles due to their increased efficiency and compactness relative to Rankine steam bottoming cycles. Since waste heat applications would be retrofits, the power system compactness is important. To achieve high efficiency, these power cycles require high pressure recuperative type heat exchangers of substantial heat duty. Current Printed Circuit Heat Exchangers (PCHE), originally developed for high pressure gas and oil applications, can be used as recuperators, but costs are higher than desired. A purpose-built high pressure and effectiveness recuperator is being developed to provide the reliability, compactness, performance and pressure capability of current recuperators, but at a reduced cost. The purpose of this effort was to analytically evaluate this design and produce and test heat exchanger test articles to determine the performance and integrity of the design.

At the outset of the effort, the waste heat based power system recuperative heat exchanger specifications were defined with the help of Echogen, a developer of waste heat based super critical CO2 power systems. Using the specifications defined by Echogen, the heat exchanger process design was defined using a proprietary heat transfer and pressure drop model. This model utilized heat transfer and friction coefficients developed from laboratory Supercritical CO_2 experiments, using small-diameter tubes consistent with the channel sizes utilized in the design. Model results covered the impact of channel height and length, hydraulic diameter, open area and number of channels on heat transfer and pressure drop performance. In addition, model results were used to calculate key heat exchanger metrics of M^3/UA and kg/UA, where M^3 is the volume and kg is the weight, and UA is the overall heat exchanger conductance, U, and total surface area, A. The calculated HELC volume, weight and cost metrics of .0024 m^3/UA, 10.2 kg/UA and $1,349/UA, were 4%, 77.3% and 10% below recuperator desired target metrics defined by Echogen. Given the potential of the design, the process parameters were then used to prepare mechanical designs for a sub-scale test article that would produce the needed performance and demonstrate the integrity and manufacturability of the design. In support of the design, SolidWorks CAD, FEA and CFD tools were utilized. To ensure integrity under expected operating conditions, the article was designed to the ASME pressure vessel code standards that included the specified safety factors.

In addition to the 50 kWt test article design, 500 kW and 5,000 kWt modules were designed that could be used as a base unit to create an array of 50,000 kW units for full-scale power plant operations. The inlet and outlet configuration of the basic design facilitates the construction of 50 module arrays that could support the 2,500 kWt recuperative heat exchanger requirements for a 400 MWe supercritical CO_2 power plant.

Using the test article design, a 50 KWt test article was fabricated using 316 stainless steel frames, plates and inserts that were bonded in a vacuum furnace, using a nickel-based braze alloy. By using braze bonding, the costs of extra surface preparation and long times under high furnace loading conditions with diffusion bonding are reduced. Following test article buildup, the HELC unit was tested using oil and water to validate the proprietary heat transfer and pressure drop model. This model was then used to predict HELC performance on supercritical CO_2 using small-diameter tube heat transfer and pressure drop correlations. These results supported the volume and weight advantages of HELC over PCHE recuperators. Following heat exchanger performance tests, the HELC was hydrostatically tested to demonstrate the integrity of the design. The first test unit developed a leak at a pressure below the

operating pressure. Investigation suggested that the leak was a result of insufficient braze amount and a lower than optimal temperature profile. After adjusting the braze amount and temperature profile, small coupon tests showed improved joint characteristics. Pressure tests of the second unit at up to 4,000 psi differential pressure showed no evidence of leaks, but it was found that the channel inserts were distorted. Investigation indicated that stress concentrations were still excessive. To alleviate these stress concentrations, the design of the inserts and manifolds were updated. It is anticipated that these design updates will improve the pressure capability of HELC to the level needed.

Based on the analysis and performance test results, the HELC design has the potential to reduce volume, weight and cost metrics versus PCHE designs. However, the pressure capability of the design fell short of the goal. The final updated design is expected to improve the pressure capability to the needed level. More development and test work is required to confirm this capability.

1.0 Introduction

Brayton power cycles that use Supercritical CO_2 ($ScCO_2$) working fluid have the potential for higher efficiency than classical Rankine based steam power cycles [1]. Furthermore, at the high pressures required for $ScCO_2$ operation, fluid densities are very high and component sizes and footprint can be substantially reduced. Given the high base pressure with $ScCO_2$, the cycle pressure ratios are limited and recuperative heat exchangers are required to maximize cycle efficiency. In the case of waste heat driven cycles, the recuperative heat duty is in the range of 100 % greater than the electrical power output, with fossil, concentrating solar and nuclear-based cycles needing 520% higher heat duties than the electrical power output. Printed Circuit Heat Exchangers (PCHE), which have been developed for very high pressure oil, gas and chemical industry heat exchanger application, have been the most widely used recuperative type heat exchangers for $ScCO_2$ power cycle development testing [2]. PCHEs are created by chemically etching small channels in thin metal plates, with an example of the construction of a counter-flow recuperative type heat exchanger using multiple stacked plates shown in Figure 1 [3].

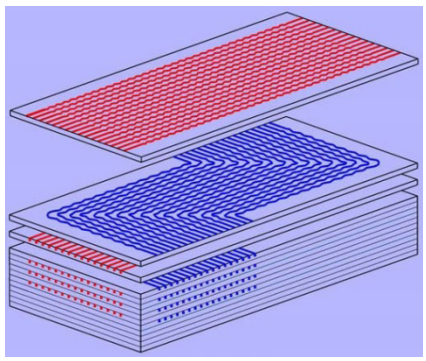

Figure 1 – Chemically-Etched Channels in Stacked Plates

For clean fluids, these channels can be created at sizes below 0.4 mm, which produces high heat transfer coefficients. To create the high heat duties needed for power cycles, many plates are stacked together and diffusion bonded in a vacuum furnace, resulting in a single block structure with thousands of channels, as illustrated by the cross-section picture shown in Figure 2 [3].

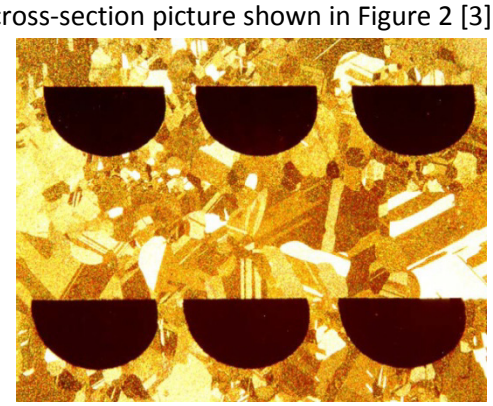

Figure 2 – Diffusion Bonded PCHE Cross-Section Picture

While robust heat exchangers can be produced for $ScCO_2$ recuperator applications, these PCHE type heat exchangers are high in cost, due to both the cost of creating chemically etched channels and

the diffusion bonding process. To effectively diffusion bond a stack of plates, the plate surface must have a high level of flatness and be cleaned of all contaminants. A high load of 4,000 psi must be applied in the furnace at temperatures that are near the melting temperature of the material for several hours [4]. This process requires stack structures of high solidity that are stable in the furnace under high temperature conditions, which is a good fit for very high pressure (e.g. 9,000 psi) oil, gas and chemical applications. However, for $ScCO_2$ power cycle applications, where 20% to 30% of the plant cost might be PCHE recuperators, lower costs are needed to improve the economic competiveness of these cycles relative to the current Rankine power cycles. To address this need, the High Effectiveness Low Cost (HELC) recuperative heat exchanger was designed for the lower peak pressure (e.g. 3,500 psi peak pressure versus 9,000 psi for oil, gas and chemical) $ScCO_2$ application. This design used materials, fabrication and bonding processes that were expected to result in lower cost at the compactness and performance levels needed to meet power cycle specifications. In the following sections, progress in HELC development and testing is reported.

2.0 Application, Goals and Specifications

The most likely first application for HELC will be 7 MWe to 10 MWe bottoming cycles driven by waste heat from industrial simple cycle gas turbines used for gas compression and other purposes. These units are at a scale and temperature that have a more acceptable risk for the introduction of new technology. Also, because waste heat is used as the energy source, fuel costs are zero and thereby the economics of thee units are favorable for early market introduction. Several companies are looking to enter this market, with Echogen being an important and early supplier to this market. Figure 3 gives a picture of their 7.5 MWe $ScCO_2$ bottoming cycle power module that can be adapted to simple cycle gas turbines, like the LM 2500 [5]. As part of their development efforts, Echogen has built small and prototype demonstration test systems that can be used to test $ScCO_2$ system components, including recuperators.

Figure 3 – Echogen Waste Heat Driven 7.5 MWe $ScCO_2$ Power Module

Echogen was contacted to review the waste heat power system application of interest and the needed characteristics of the HELC internal heat exchangers. The primary application will be the many multi-megawatt scale simple cycle gas turbines used in industry, and particularly the oil and gas industry. These units have exhaust temperatures of over 1000F and represent good candidates for recovering high value energy typically exhausted to the atmosphere. Prior to deploying HELC technology on full-scale

systems, sub-scale prototypes will be developed and demonstrated to prove the technology. Tables 1 and 2 provide specifications for 30 kWt laboratory and 500kWt demonstrator test units, respectively.

Table 1 - 30 kWt HELC Specifications for Laboratory System Tests

Lab system recuperator (0.4 kg/s)						
	SERVICE PER ITEM		SIDE A		SIDE B	
1	FLUID CONDITIONS		In	Out	In	Out
2	Fluid		LP Carbon Dioxide		HP Carbon Dioxide	
3	Flow rate, total	kg/s	0.4		0.4	
4	Flow rate, gas/vapor	kg/s	-	-	-	-
5	Flow rate, liquid	kg/s	-	-	-	-
6	Temperature	ºC	138.0	43.5	31.5	70.3
7	Design temp: max/min	ºC	200 / -29		200 / -29	
8	Pressure: inlet/design	Mpa	6.5 / 11.03		14.5 / 20.0	
9	Allowed Pressure drop:	MPa	0.1		0.1	
17	No. of nozzles		1	1	1	1
18	Nozzle	mm NB	25.4 (1") Swagelock	25.4 (1") Swagelock	25.4 (1") Swagelock	25.4 (1") Swagelock
19	Flange class					
27	Design heat load	kW	49.7	LMTD	°C	32.2

Table 2 – 500 kWt Specifications for Demonstrator System Tests

Demo system recuperator									
	SERVICE PER ITEM		SIDE A				SIDE B			
1	FLUID CONDITIONS		In		Out		In		Out	
2	Fluid		LP Carbon Dioxide				HP Carbon Dioxide			
3	Flow rate, total	kg/s	6.56				6.56			
4	Flow rate, gas/vapor	kg/s	-		-		-		-	
5	Flow rate, liquid	kg/s	-		-		-		-	
6	Temperature	ºC	99.7		44.4		38.9		70.6	
7	Design temp: max/min	ºC	343 / -29				200 / -29			
8	Pressure: inlet/design	Mpa	6.2 / 10.3				20.7 / 23.2			
9	Allowed Pressure drop:	MPa	0.07				0.07			
10	FLUID PROPERTIES		Liq	Vap	Liq	Vap	Liq	Vap	Liq	Vap
17	No. of nozzles		1		1		1		1	
18	Nozzle	mm NB	64 (2.5") C1 1500 RTJ		64 (2.5") C1 1500 RTJ		76 (3") C1 900 RTJ		76 (3") C1 900 RTJ	
19	Flange class		ASME B16.5 flange		ASME B16.5 flange		ASME B16.5 flange		ASME B16.5 flange	
27	Design heat load	kW	497.3		LMTD		°C		14.2	

Figures 4 and 5 are pictures of the 30 KWt and 500 KWt test systems, respectively.

Figure 4 – Echogen 30 KWt Test System

Figure 5 – Echogen 500 KWt Test System

3.0 Full-Scale and Test Article Designs

HELC is a layered counter-flow heat exchanger comprised of alternating plates and frames, as illustrated in the preliminary design given in Figure 6. This classical counter-flow arrangement gives high effectiveness levels that are important to the $ScCO_2$ cycle performance. As shown in Figure 6, the frames have alternating inlet and outlet port locations on the ends, which yield roughly equal length channels. The inlets and outlets for the high and low-

pressure sides are mirror images as viewed in Figure 6. However, the frame that contains the inserts that form the channels can have different thicknesses to accommodate the different densities and velocities between the high and low pressure layers in the heat exchanger. To provide flow guidance, strength and enhance heat transfer at an acceptable pressure drop, a special insert is included inside the frames for both high and low pressure layers. To address an application of interest, a single channel configuration and length is optimized for the needed heat transfer performance within the specified pressure drop. The needed heat duty is then achieved by a multiplicity of channels and the associated manifolding to accommodate the inlet and outlet flows. While minimal volume and weight can be defined based on heat transfer and pressure drop physics, practical constraints related to channel corrosion and plugging by contaminants, overall system space claim and manufacturing limitations must also be considered in the design.

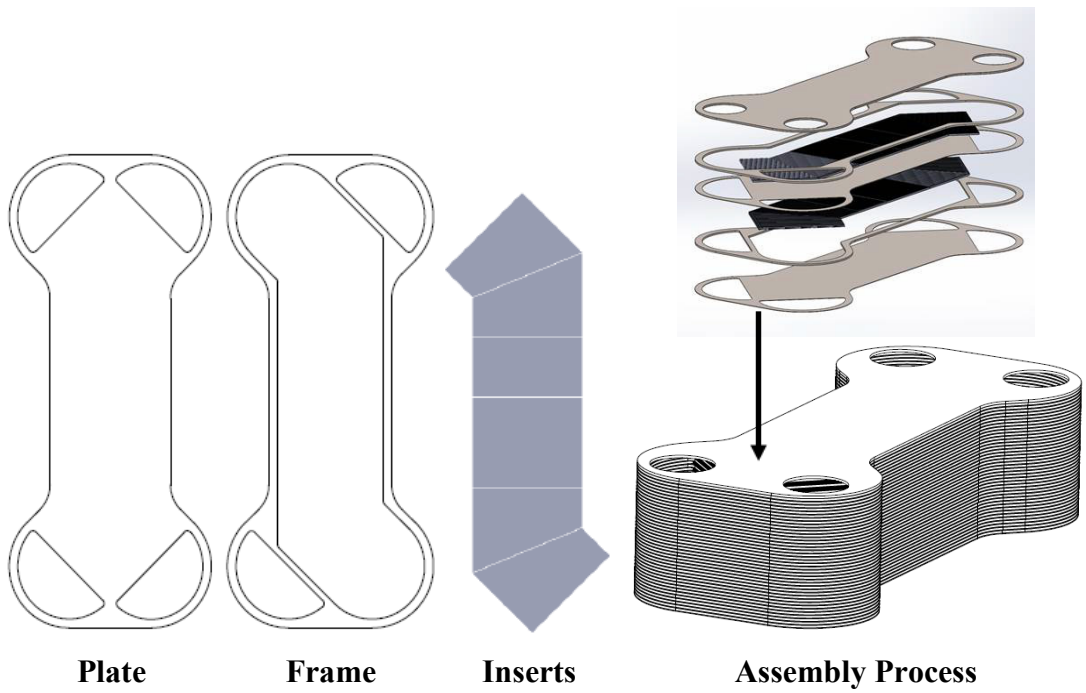

Figure 6 – HELC Preliminary Design Basic Plate and Frame Geometry

In support of designing HELC, a model that captures the heat transfer and pressure drop characteristics as a function of key parameters was needed. Given the repeating small linear channel configuration of HELC, as illustrated in Figure 6, and the complexity of the $ScCO_2$ fluid, a well-proven J and F-based model was selected for use under this effort [6]. These models use correlations of J (Colburn modulus) and f (friction factor) data obtained on similar geometries and at similar conditions. The models include heat transfer and energy balances, as well as pressure drop relationships, that cover wall friction, entrance, exit and acceleration contributions to pressure drop. This method has been extensively used in compact heat exchanger design, particularly with gaseous fluids [6]. However, care has to be applied in using the model with $ScCO_2$ because fluid properties can vary significantly around the critical point [7]. In these cases, the model can be broken into multiple along the channels segments where fluid properties are relatively constant across the segment. With this approach, the accuracy of these simple

models can be improved to the needed level. The available proprietary Altex HELC J and f-type heat exchanger model was updated and utilized to define HELC performance as a function of important design parameters. The model incorporates heat transfer and pressure drop correlations for ScCO2 flowing in mini/micro channels [8]. The heat transfer model includes buoyancy effects (Grashof number, Gr, related) driven by density differences, even with high Reynolds number flows. These buoyancy effects create secondary flows that drive up the heat transfer for cases where Gr/Re^2 is greater than .001 [8]. For small diameter tubes where Gr/Re^2 is less than .001, the secondary flows are weak, and the heat transfer coefficient becomes consistent with a Dittus-Boelter correlation [8]. As introduced above, variable specific heat is considered in the model by "slicing" the channel length into several segments where each segment uses constant properties. These segments are linked together to predict heat transfer and pressure drop over the length of the heat exchanger. Wall friction, core entrance, exit and flow acceleration pressure losses are included in the overall pressure drop calculation for the Altex model. However, the manifold flows are complex and these are estimated through SolidWorks Flow CFD model calculations [9]. Conduction heat transfer within the solid core structure is included in a simplified way, using a heat transfer area effectiveness factor. This approach is taken to be able to rapidly run multiple cases to optimize key design parameters for the operating conditions of interest.

The counter-flow portion of HELC drives the heat transfer performance of the design. At either end of the heat exchanger, a short portion contains a crossflow region required to create separation of flows for the high and low pressure inlet and outlet manifolds. These cross-flow zones will contribute to heat transfer. However, to be conservative in the design, the contribution to heat transfer by these zones is assumed to be negligible.

As given in the specifications listed in Tables 1 and 2, the HELC performance requirements are tightly specified. Furthermore, while not presented herein, there are geometrical constraints on the overall heat exchanger, if the HELC is expected to be retrofitted to the existing demonstrator power system that previously utilized a Heatric microchannel heat exchanger. In addition, while optimal performance might be achieved by a long length core, manufacturing constraints, particularly the bonding furnace dimensions, could limit core length. Lastly, it is anticipated that channels with smaller dimensions will yield higher heat transfer coefficients. Smaller channels could then reduce the flow length required for a given heat transfer. However, the minimum channel hydraulic diameter is limited by the cleanliness of the fluid and any potential long-term corrosion that could block channel flow. Therefore, for long-term operation, channel hydraulic diameter should be larger than 0.7 mm for the application of interest. Given all of these constraints, HELC individual channel heat transfer and pressure drop performance will be governed by channel length and velocity. With a fixed total mass rate from the specifications, the setting of channel velocity then defines the number of channels to achieve the needed heat duty. Assuming that the bonding furnace would limit core length, the different heat duty requirements (e.g. 30 kWt, 500kWt, 15,000 kWt) would then be met by changing the number of channels. From a performance perspective, the number of channels in the horizontal direction versus those in the vertical direction is not important, and the core width to height ratio can be varied to fit the application. Packaging and manifold constraints will limit this ratio. Reducing the core width will increase the height for a given heat duty. Given that inlet and outlet manifold width will be constrained by the core width, core width must be large enough to provide sufficient manifold flow area to limit manifold flow velocity, and thereby flow non-uniformities and pressure drop.

For large heat duty applications, the core size could be constrained by common sizes of raw materials and bonding furnace dimensions. With even the largest bonders, as illustrated in Figure 7, the

platen that applies pressure to the stack and thereby stack dimension is limited to about sixty-inches. In these cases, the heat exchanger cannot be manufactured in a single unit and multiple cores would then need to be fabricated and linked together in parallel by welding on secondary manifolds. While these comments are brief, they point out some of the important constraints and free parameters that govern heat exchanger design.

Current compact high-pressure heat exchanger performance metrics for $ScCO_2$ recuperators have been established. According to Echogen, a competitive heat exchanger for the waste heat application of interest should have core volume, weight and cost metrics of .0025m^3/UA, 45kg/UA and $1500/UA, respectively for a 500 KWt heat exchanger, where UA is the fluid conductance multiplied by the heat transfer surface area [2]. The available model was used to evaluate the capability of HELC to meet or exceed these metrics.

As noted above, smaller channel hydraulic diameters will increase the heat transfer coefficient and increase heat transfer. However, for the constrained system, some performance parameters can be impacted in unexpected ways. Table 3 presents results for fixed channel velocities and core width, with individual channel height decreased to reduce the hydraulic diameter, dh. As shown, reducing the dh increases heat transfer, Q. As dh is reduced, the number of layers, and part count, increase by a factor of three to maintain the same channel velocity. Because the core now has three times the number of plates, the overall core height is increased and the free flow area is reduced. Therefore, while the reduced dh and channel height improves heat transfer by 10%, the overall height increases by 39%, and the part count increases by a factor of three, with a corresponding increase in forming operations and bonded joints. Relative to the m^3/UA and kg/UA metrics these decrease by 15.4% and increase by 8.6%, respectively. This opposite behavior is a result of the relative changes in conductance and surface area versus overall volume and weight, the latter being impacted by the decreasing free flow area versus total face area as dh decreases. These results show the complexity of the constrained problem, and that care has to be applied in optimizing the design for key variables. Of note is that for a channel height of 0.2375 inch, the key metrics are .0024 m^3/UA and 10.2 kg/UA, or 4% and 77.3% below the Echogen-defined targets noted above. This shows the potential of the HELC design.

Table 3 – Variation of HELC Performance and Geometrical Parameters with Hydraulic Diameter Reduction

CHANNEL							
HEIGHT	DH	Q	LAYERS	HEIGHT	FREE AREA/		
IN	MM	KW		IN	AREA	M3/UA	KG/UA
0.3	1.69	488	16	12.28	0.60	0.0026	10.5
0.25	1.66	499	20	12.76	0.57	0.0024	10.2
0.2375	1.65	502	21	12.92	0.57	0.0024	10.2
0.2	1.60	511	25	13.49	0.54	0.0023	10.2
0.15	1.52	523	33	14.69	0.50	0.0022	10.4
0.1	1.39	536	49	17.09	0.43	0.0022	11.4

Performance predictions using the HELC heat exchanger model showed that core volume and weight are reduced as the core counter-flow channel length is increased, as illustrated in Table 4. In these

calculations, for the fixed channel geometry and mass flow of 6.56 kg/sec, the velocity was increased as flow length was increased to maintain the same effectiveness and heat transfer of 500 kWt. Of course, with increasing length and velocity, the pressure drop increased substantially, as shown in Table 4. However, maximum pressure drops were within the limit of 15 psi. Besides volume and weight, the number of channels, or layers, is reduced by a factor of five as channel length is increased. This reduces part count for a given heat transfer. Since part count and weight relate to cost, a longer channel design should be lower in cost. Performance metrics, m^3/UA and kg/UA also decreased substantially with length, with Table 4 showing reductions of 34.4% and 27.7%. These reductions should be beneficial to packaging and costs. Importantly at a core length of 54 inches, the m^3/UA and kg/UA parameters are 16% and 79.1% below the Echogen-defined metrics. At a shorter length of 36 inches, the m^3/UA and kg/UA parameters are 4% and 77.3% below the Echogen-defined metrics. Again, this supports the potential of HELC to meet the desired target metrics for an improved recuperator versus the PCHE.

Table 4 – Variation of HELC Performance with Increases in Channel Length

				COLD	HOT	CORE	CORE		
LENGTH	HEIGHT	NUM	Q	DELP	DELP	VOL	WEIGHT	M3/UA	KG/UA
IN	IN	LAYERS	KW	PSI	PSI	CF	LB		
17.7	36.9	59	501	0.02	0.12	3.49	887.18	0.0032	13.0
27.6	19.1	31	501	0.09	0.70	2.89	752.75	0.0026	11.0
36.0	12.9	21	501	0.24	1.96	2.61	693.21	0.0024	10.2
45.6	9.1	15	500	0.62	4.99	2.39	651.60	0.0022	9.7
54.0	7.1	11	500	1.17	9.49	2.29	636.73	0.0021	9.4

Simultaneous to the performance modeling efforts, the HELC mechanical design, as illustrated by the basic layout in Figure 1, was developed using SolidWorks. The general design approach was to use a full brazed construction consisting of fluid separation plates, with frames to contain special inserts and provide strength to oppose pressure forces at the required pressure differentials. Preliminary designs were prepared for the 32 kWt unit that was expected to serve as a base for a 500 kWt unit. To achieve the higher heat duty, the 500 kWt unit will have many more layers than the 32 kWt unit.

As noted above, within the specified pressure drop constraint, longer channels reduce volume and weight for a given UA (i.e. conductance multiplied by heat transfer surface area). For large heat duty applications, the core size will potentially be constrained by bonding furnace dimensions. To address this limited core length for high capacity applications, the HELC manifold configuration was revised as given in Figure 7. Another benefit of this configuration is that the higher pressure and lower velocity pressure drop fluid can negotiate the right angle turns at the ends of the heat exchanger, with the higher velocity and pressure drop fluid channels utilizing straight channels. This configuration better balances heat transfer and pressure drops.

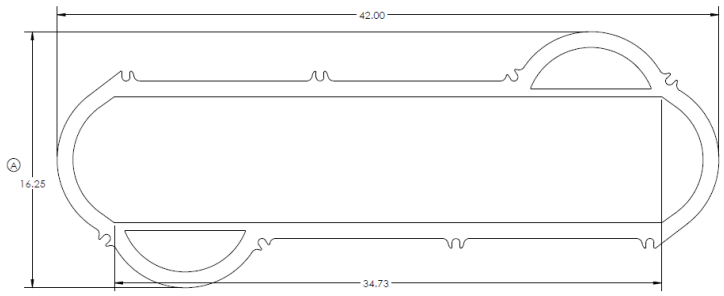

Figure 7 – Revised HELC Frame Configuration Example

Another advantage of the revised configuration, shown in Figure 7, is that the inlets and outlets on each end are now offset. This allows full-scale modular units to be closely spaced with external pipe manifolds that will link modules together in parallel to meet utility-scale heat transfer capacity needs. To illustrate this feature, Figure 8 gives a picture of a 50 kWt HELC test article to the right and illustrations of a 50 MWt HELC module to the left and an array of 50 modules with connecting pipes that yield a 2,500 MWt recuperative heat duty that would be needed for a 400MWe power plant. It should be noted that the footprint of the array is only 3.5% of a dry cooling condenser for a comparable 400 MWe capacity steam power plant.

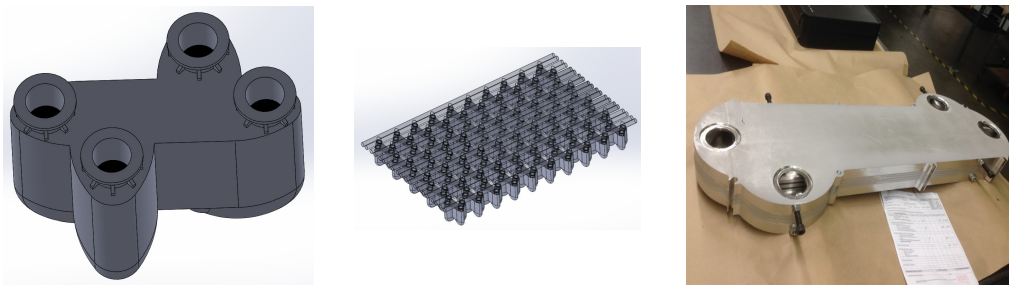

50 MW Module **50 Module Array** **50 kW Test Article**

Figure 8 – 50 MWt and 50 Module Array with 50 kWt Test Article

Using the refined HELC approach, the 50 kWt test article final design was produced, as illustrated in Figure 9, with the actual article shown to the right in Figure 8 above. The figure shows the layered counter-flow HEX configuration, including top and bottom plates.

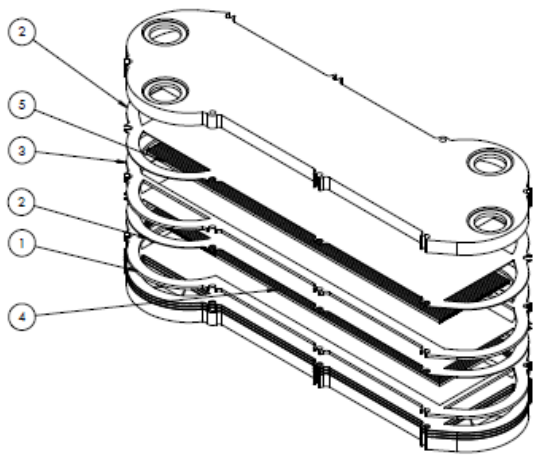

ITEM NO.	PART NUMBER	Revision	Description	QTY.
1	667-101	A-02	HP Frame	2
2	667-103	A-02	Plate 42	5
3	667-102	A-02	LP Frame	2
4	667-104 mockup	A-01	HP insert	2
5	667-104 mockup	A-01	HP insert	2
6	667-122	A-03	Top Inner Endplate	1
7	667-123	A-03	Bottom Endplate	1

Figure 9 – Final 50 kWt HELC HEX Mechanical Design

Once the unit is bonded in the Vacuum Process Engineering (VPE) vacuum furnace, inlet and outlet connection bosses and gusset stiffeners are welded on the top plate, as illustrated in Figure 10. These gussets are needed to provide stiffness to the open manifold areas outside of the core. The FEA results presented in Figure 10 indicate that the stiffeners have added sufficient strength to limit local stresses to below the 12.4 ksi allowable stress as determined from the ASME Pressure Vessel Code (PVC) for 316 stainless steel at the temperature conditions of interest [10]. It should be noted that a detailed FEA of the complete HELC HEX indicated that all areas have stresses below the 12.4 ksi allowable stress for the 316 SS construction material.

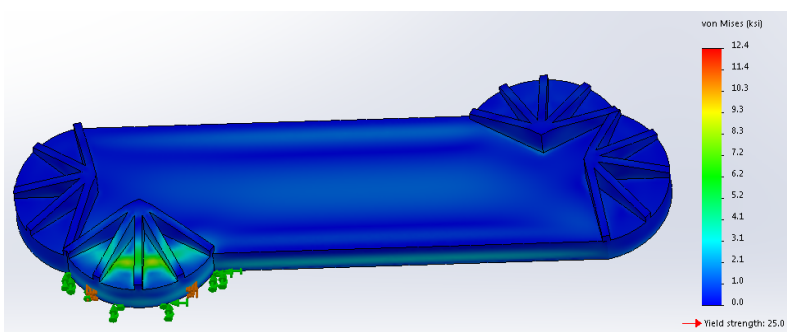

Figure 10 – Finite Element Analysis Showing Stresses in HELC Bottom Plate Under Operating Conditions of Interest

4.0 Heat Transfer Enhancement

The initial HELC test article will utilize smooth and straight channels of small hydraulic diameter that promote high heat transfer at acceptable pressure drop. Using this approach, the HEX is compact and low weight versus a HEX that uses larger hydraulic diameter channels. However, it is of interest to enhance heat transfer to further reduce volume and weight that will lead to even lower cost. For the channel dimensions of interest, the use of dense $ScCO_2$ results in turbulent transition flow within the

channels. Under these conditions, channel features can be introduced to enhance heat transfer. This approach has been incorporated into other micro/mini channel heat exchangers, including the Heatric HEX [11]. In a number of applications, a wavy channel configuration, as illustrated in Figure 11, is utilized. While this enhances heat transfer as the flow separates at the wave peaks, the large disturbance to the flow at this location also substantially increases pressure drop.

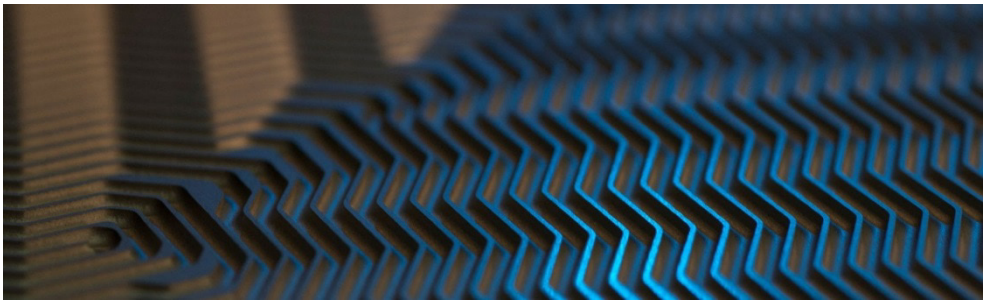

Figure 11 – Mini-channel Wavy Channel Wall Configuration Example

To provide a more balanced approach, the HELC special channel features enhance heat transfer but avoid large-scale flow separations that drive up pressure drop. In this case, the high thermal efficiency (i.e. heat transfer versus flow energy needed to drive heat transfer) of a straight and smooth channel is maintained. This high thermal efficiency translates into higher overall power production efficiency by reducing parasitic power losses due to HEX pressure drop. This is particularly important for $ScCO_2$ Brayton cycles, where internal recuperative heat exchangers have large heat duties and significant pressure drops. To illustrate the heat transfer enhancement effect using the special HELC channel features, Figure 12 presents a comparison of the Colburn J factor versus Reynolds number based on the channel hydraulic diameter and velocity. This J factor is utilized with other parameters to define the heat transfer coefficient. A higher J gives a higher heat transfer rate. As shown, in the turbulent transition range of interest, approximately 100% heat transfer enhancement can be achieved with the special channel features. Of course, pressure drop is increased, but not as much as with wavy channels.

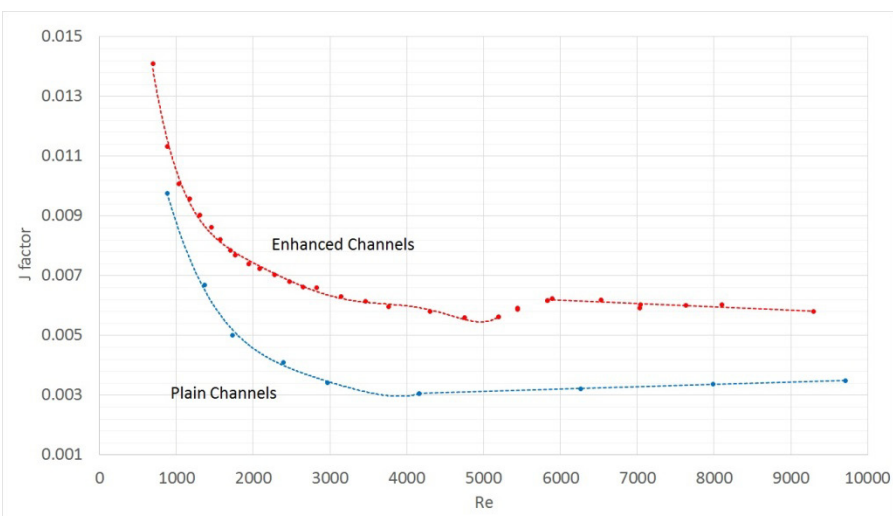

Figure 12 – Comparison of Colburn Heat Transfer Coefficients For Smooth and Straight Channels versus HELC Enhanced Channels

5.0 Test Articles and Performance and Integrity Testing

The 50 kWt test article is useful for testing the integrity and performance of the overall HELC design approach. However, the capacity is substantially below the planned 15 MWt type requirement of the full-scale system. As an intermediate HELC demonstrator scale, the 50 kWt test article design was adapted to the 500 kWt demonstrator HEX. To meet this order-of-magnitude higher heat duty, the number of channels, or layers, used in the 50 kWt design is expanded by a factor of ten. This increases the height of the HEX by approximately a factor of ten, with the width and length remaining relatively constant. Figure 13 presents the design of the assembled 500 kWt HELC that leverages the design of the 50 kWt shown in Figure 9. By carrying over most of the 50 kWt design features to the 500 kWt design, except for the number of layers and height, the performance and integrity risk for the larger heat exchanger are reduced.

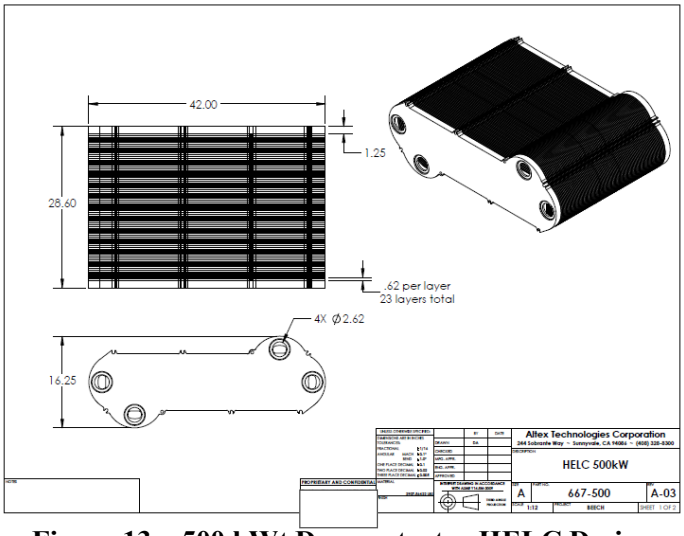

Figure 13 – 500 kWt Demonstrator HELC Design

After reviewing the acceptability of the 50 kWt design with VPEI, the braze bonding process was finalized and parts needed to build this small test unit were acquired, including inserts, plates and frames. These parts were stacked and bonded to create the HELC module. Figure 14 provides pictures of some of the parts. Following bonding, the unit was leak checked using a standard helium method applied by VPE. The unit was then hydrostatically tested at Altex.

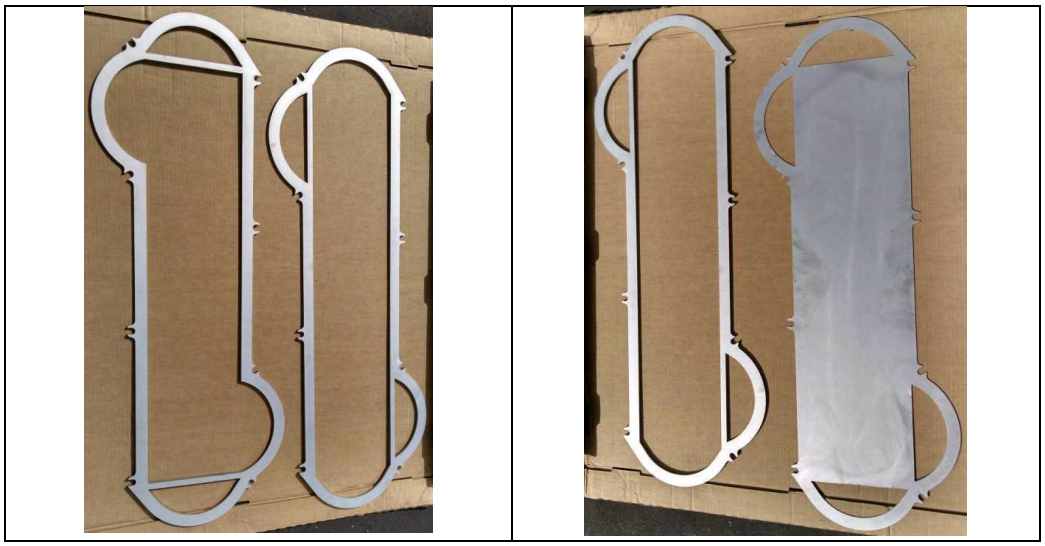

Figure 14 – 50 kWt Frame and Plate HELC Parts

The heat exchanger was designed to pressure vessel code allowable stress limits of 12.5 ksi for 316 stainless steel material at a maximum design temperature of 650F. This is the temperature defined by Echogen for their waste heat power generation application of interest. This is the maximum design temperature for the hot side gas, as listed in Table 1. The maximum design differential pressure is 2745psi, considering the 3365psi on the cold side and 1494psi on the hot side listed in Table 5.

Table 5- Heat Exchanger Design Conditions

Design Conditions	Low Pressure Side	High Pressure Side
Temperature (max)	650F	392F
Pressure (min/max)	899psi / 1494psi	3002psi / 3365psi

From the Pressure Vessel Code ASME Section VIII – Div I UG-99(b) the hydro static test pressure is calculated by taking the maximum design pressure multiplied by a safety factor, and then multiplied by the lowest stress ratio for the temperature difference in operation versus the cold hydrostatic testing. The safety factor is 1.3 and the temperature correction is given in Table 6 below.

Table 6 – Code Factor for Operating Temperature Effect

Temperature (F)	100	200	300	400	500	600	650
LSR factor	1.000	1.156	1.282	1.399	1.504	1.587	1.626

This factored pressure was utilized in the 50 kW test article FEA model and results of the analysis show that the maximum stress for the inserts reaches 33ksi. Since the material certifications for the inserts have

a 40ksi yield stress, operating the article at this test pressure will not cause the stress to exceed the yield stress of the 316 stainless steel material. However, the joints are formed from a high nickel braze compound that has different strength characteristics than the 316 stainless steel. At room temperature, the joint material could have a joint strength 75% to 85% of the base material [12]. However, at higher temperatures, the nickel-based joint material has a strength that approaches the base material strength. As an example, Figure 15 gives the braze strength versus 316 stainless steel strength at room temperature and at 910 C [12]. As shown, the strengths are nearly the same at the higher temperatures. This supports using the 316 stainless steel properties in the FEA model.

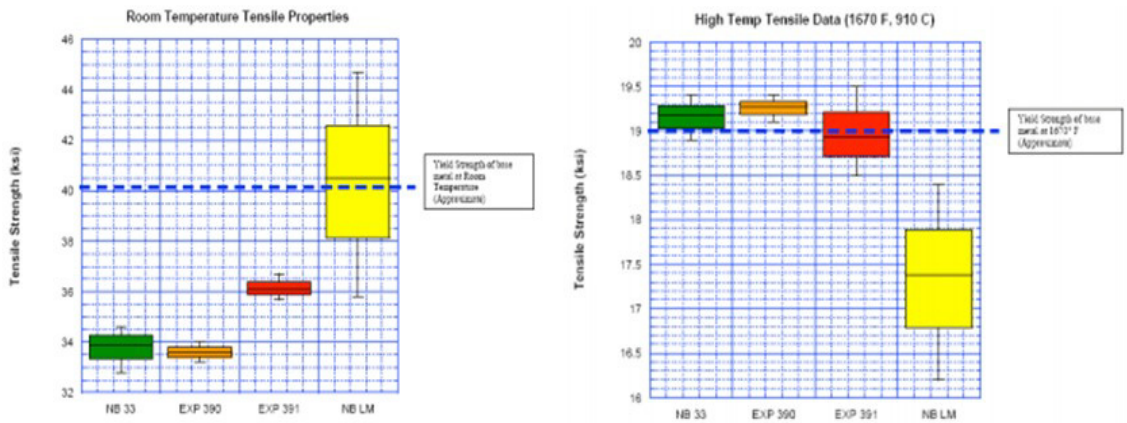

Figure 15 – Comparison of 316 Stainless Steel and Nickel Braze Strength

The maximum stress determined by the FEA analysis is 12.5 ksi. The actual operating temperature of the heat exchanger is 212F, which from the codes has an allowable stress of 17.5ksi. This means there is a 1.4 safety factor to the pressure vessel code allowable stress, and 3.2 safety factor to yield, and a 7.4 safety factor (92.6ksi/12.5ksi) to the tensile stress limit of the material. Given that the 50 kWt design was shown to meet the pressure vessel codes and was found to be acceptable to VPEI for manufacture, parts needed to build this small test unit were acquired, including inserts, plates and frames. For this first article, the nickel-based braze compound was plated on the separating plates to an approximate 0.002 inch thickness. The plating would provide braze to both the joints on the frames and inserts. After confirming that the parts met tolerance specifications, the parts were stacked and bonded into a HELC using a baseline furnace loading and temperature history for nickel-based brazing of 316 stainless steel parts.

The left side of Figure 16 gives a picture of the bonded unit. Following bonding, the unit was leak checked using a standard helium leak detection method. It was found that the unit leaked at joints around the periphery. The right side of Figure 16 gives a picture of the periphery, which shows that the braze compound did not flow as much as expected. More detailed inspections of the joints indicated that the amount of braze may also have been insufficient to create leak free joints, in addition to the standard temperature profile being too low to get good braze flow at the joints. Strategies were then developed to correct the braze quantity and temperature profile to improve joint quality. To check the improved approach ahead of bonding the next HELC, some coupons were tested. The top of Figure 17 shows the bar and plate coupon that was processed at the same temperature as the initial HELC test unit. As shown, the joint has a similar appearance to the HELC edge picture in the right of Figure 16. In the lower part of

Figure 17 is pictured the coupon that was brazed using a higher temperature furnace profile. As shown, there is more braze flow for this temperature profile, as evidenced by the wider region of braze flow away from the joint. It was expected that this profile would provide better joint sealing and strength for the HELC unit. Using the improved temperature profile and more braze compound the second test article was successfully bonded, and the helium test showed that the unit had no leaks,

50 kWt First Test Unit	50 kWt First Test Unit Edge Image
	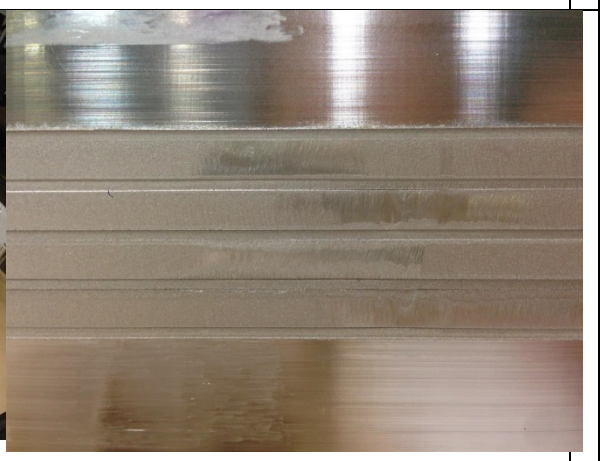

Figure 16 – 50 kWt First Test Unit

Figure 17 – Test Coupons Brazed at Lower (top) and Higher (bottom) Furnace Temperatures

This unit was then performance tested at Altex using water as the working fluid, rather than supercritical CO_2. The purpose of these tests was to show the validity of the HELC model by comparing predicted performance with water to test results. Figure 18 compares the predicted and measured heat transfer results. As shown, over the conditions tested, the predicted results are within 17% with the

results at the highest water flow within 1.5%. It should be noted that heat and pressure drop correlations for water are well known relative to $ScCO_2$ correlations.

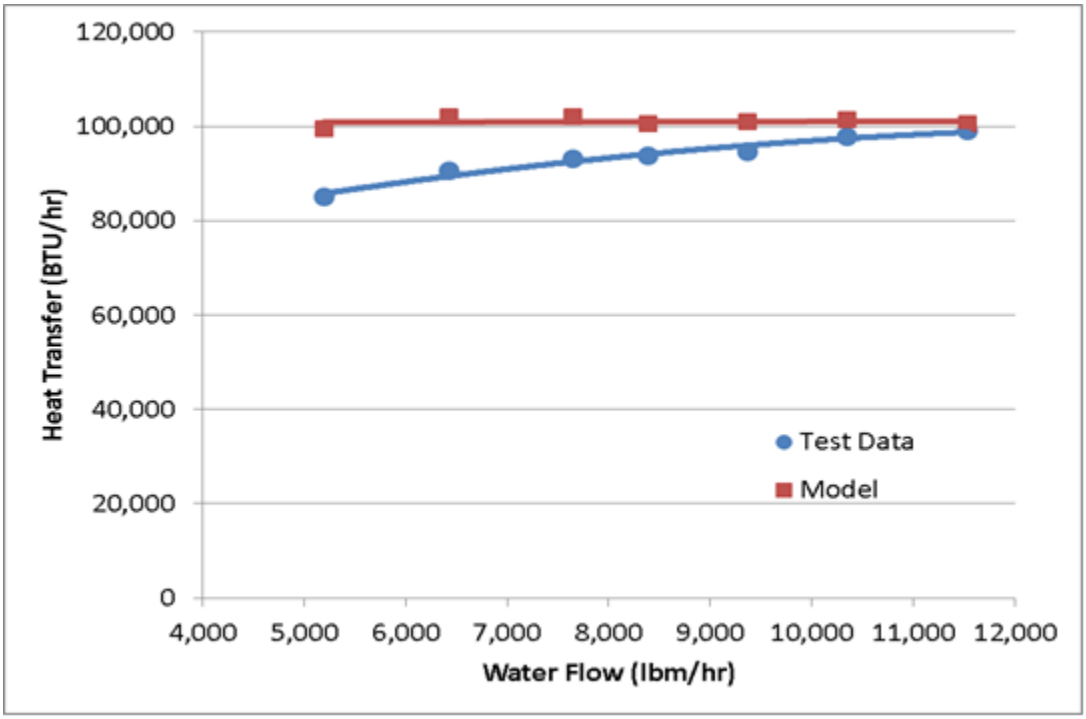

Figure 18 – HELC Predicted versus Measured Heat Transfer Results

For example, the rapid change of $ScCO_2$ density with temperature around the critical point can create secondary flows in channels that require the inclusion of Grashof number effects in the correlations [8]. These buoyancy-driven secondary flows, and related heat transfer impacts can be significant in large hydraulic diameter channels. However, with the very small and non-circular channels used in HELC these secondary flows and impacts will be limited. With reduced buoyancy effects, the extra parameters needed to be input into the correlations will be reduced. This should reduce the uncertainty of the correlations and improve the accuracy of the results.

For HELC predictions, available laminar and turbulent correlations for J and f factors for water flow were utilized. These are well-proven correlations that have been utilized by Altex in prior efforts. The correlations consider flow in single channels with the overall model considering multiple counter-flow channels. The complicating effects of axial heat conduction in the metal matrix and cross-flow effects at the ends of the heat exchanger, which are needed to link the channels with the inlet and outlet manifolds, are not considered in the model. For the 50 kWt type unit tested, only one layer (one high pressure flow and one counter-flow low pressure flow channels) was fabricated with thick 1.5-in end plates, as illustrated in Figure 16. In this case, the axial heat conduction is more significant. Also, with only a single layer, the main channel heat transfer is only through one fluid separation plate. For multiple layer and larger capacity heat exchangers, each channel would have two separation plates and the effect of conduction in the thick end plates would impact only a few of the many channels. In these larger capacity cases, the simple model and test results should be aligned. However, corrections are needed to align the 50 kWt model and test results.

The primary correction for the 50 kWt case was to limit heat transfer in the model to that for the single separation plate, which decreases the effectiveness of the conduction heat transfer in the insert webs. Relative to axial conduction in the end plates, the impact on heat exchanger effectiveness is less than 1% at the modest channel heat transfer rates of interest, and no correction was included for this

effect. Given the external surface area relative to the heat duty of the single layer article, external heat transfer can be an issue. During tests the unit was insulated with low weight and low conductivity fiber insulation material, and the heat loss versus heat input was estimated to be approximately 10%. Using the correction factor for the single separation plate, the test data were compared to the corrected model results in Figure 18. As shown, the heat transfer predicted by the model is fairly constant over the range of water flows measured. As is well known, under turbulent flow conditions, heat transfer will increase with water flow. However, in the current tests, the peak water temperature decreased as the water flow increased. This reduced the temperature driver for heat transfer at the higher water flows, offsetting the flow effect and resulting in the nearly constant heat transfer rates over the water flows tested. Compared to the test data, test results at a flow rate of 11,535 lbm/hr were within 1.5% of the predicted results, as indicated in Figure 18. However, at the lowest flow rate of 5,193 lbm/hr, the test and model results are 17% different. It should be noted that the water case had cold side Reynolds numbers that covered the turbulent transition zone as the water flow increased. As is well known, it is very difficult to model transition flows with simple models, and small disturbances could lead to earlier transitions. Therefore, the differences in the heat transfer results shown in Figure 18 are not unexpected. Based on the performance test results, it was concluded that the heat exchanger model can be used to predict HELC heat transfer and pressure drop performance to the limit of the $ScCO_2$ correlations for heat transfer and pressure drop in small diameter channels. This supports the design parameter results included in Tables 3 and 4. Also, as noted in the Full-Scale and Test Article Designs section, the model results for $ScCO_2$ showed that the HELC would reduce the heat exchanger volumetric and weight metrics by 4% and 77.3% relative to the system developer desired targets, as summarized in Table 7. These are important advantages for HELC that can result in cost savings driven by the reduced amount of materials to obtain a given heat transfer.

Table 7 – Comparison of HELC and PCHE Volume and Weight Metrics for

Heat Exchanger Type	$m^{3/}UA$	Kg/UA
System Developer Targets	**.0025**	**45**
HELC	**.0024**	**10.2**
HELC Reductions	**4%**	**77.3%**

Besides performance testing, the heat exchanger was tested for maximum pressure capability. Figure 19 gives a picture of the pressure test setup with the welded on inlet and outlet fittings. The weld beads were close to the brazed joints around the periphery of the manifolds, but the welding process did not disturb the brazed joints. To test the unit, the high-pressure channels were pressurized with water. Water was pumped through the lower pressure channels and pressure drop for a fixed flow was measured to determine channel distortion as a function of pressure. As the low-pressure channels distort and become smaller in cross section, the flow area is reduced and pressure drop increases due to the channel velocity increasing.

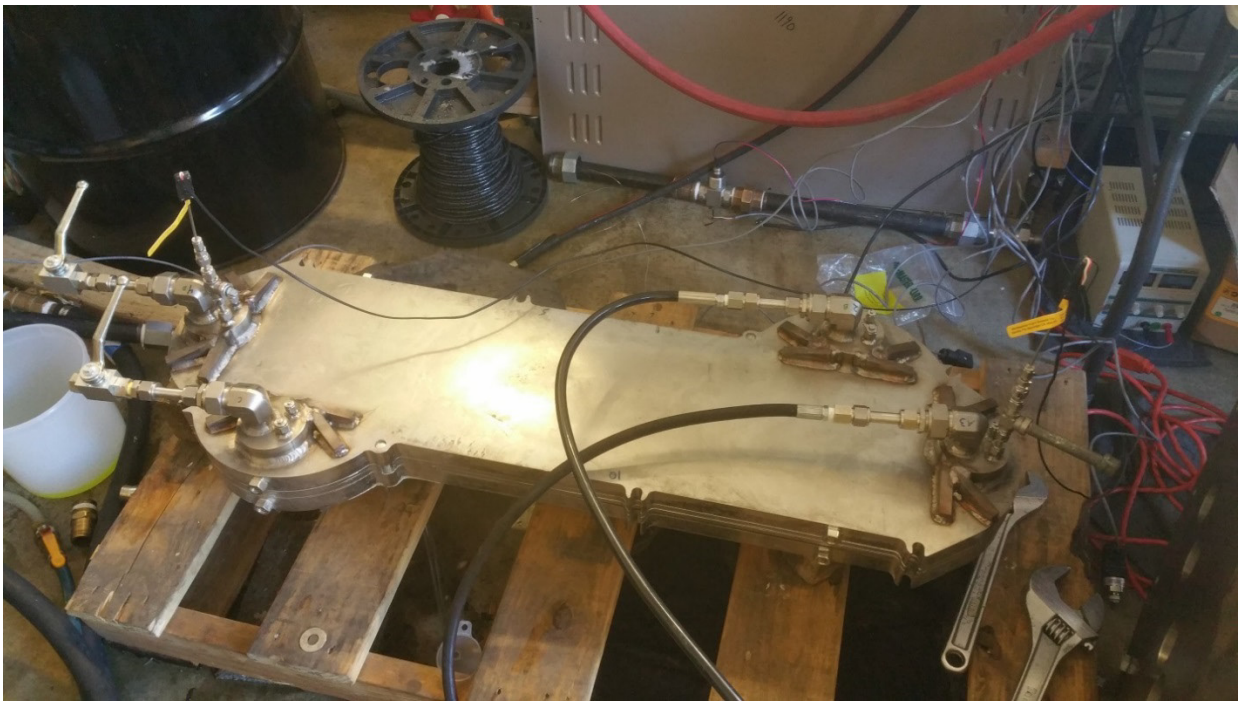

Figure 19 – HELC HEX Pressure Test Set-up

The maximum design differential pressure is about 2,500 psi; however, pressure tests are needed at higher levels to prove heat exchanger integrity. A pressure differential of 4,000 psi was tested without leakage. However, channel flow tests showed that they were deformed at the high differential pressure. To determine the extent and mechanism of distortion, the unit was sectioned and examined.

Based on inspection of the sectioned parts and joints, summary conclusions were reached and these are listed in Table 8 along with recommended actions, as required.

Table 8 Pressure Test Summary Results

Item	Result	Mitigation
Manifold	Withstands 4,000 psi without leakage and distortion	None required
Core boundary edges	Withstands 4,000 psi without leakage and distortion	None required
Core braze joints	Limited faying surface noted where insert joints were compromised	Insert designed with more faying surface and braze material
Core insert	Insert compressive stress on the low- pressure side distorts insert	Insert designed with more insert web thickness to reduce stress and distortion

Using FEA analysis of the as built and tested unit, it was found that insert web and joint stresses were higher than that for an ideal configuration, as a result of bending stresses near the braze joints. Based on these results, the insert design was refined to reduce bending stress and web sections and webs per inch were increased to further lower stress on the web and joints. Table 9 summarizes the web and joint stresses for different webs per inch and web thicknesses for the 2500 psi channel-to-channel pressure differential of interest. The hydraulic diameter for each case is also given. The lower the hydraulic

diameter, the higher the heat transfer coefficient and pressure drop. The tested configuration used 0.008-inch thick webs at 26 webs-per-inch. As shown in the table, the web stress is below the allowable stress of 16.6 ksi as per ASME Section VIII pressure vessel code for 316 stainless steel at the temperatures of interest. However, for 20 webs-per-inch, the .008-inch web stress is close to allowable stress. As the web thickness is increased, the web stress for the same pressure differential is significantly reduced. If it is conservatively assumed that every other 16 ksi web joint is poorly bonded, then the allowable stress would be approximately half the 16.6 ksi, or 8.3 ksi. In this very conservative limit, Table 9 shows that web thicknesses of .008-inch, .012-inch and .012-inch, or greater, would be viable for 30, 26 and 20 webs-per-inch, respectively. Relative to hydraulic diameter, the thicker webs would have better heat transfer, particularly with higher webs-per-inch.

Table 9 – Insert Web Stress for Different Webs-Per-Inch and Web Thickness

WEB THICKNESS IN	WEBS PER INCH	CHANNEL WIDTH IN	WEB STRESS KSI	DH IN
0.008	30	0.025	7.917	0.046
0.012	30	0.021	4.444	0.039
0.015	30	0.018	3.056	0.034
0.02	30	0.013	1.667	0.025
WEB THICKNESS IN	WEBS PER INCH	CHANNEL WIDTH IN	WEB STRESS KSI	DH IN
0.008	26	0.030	9.519	0.054
0.012	26	0.026	5.513	0.048
0.015	26	0.023	3.910	0.043
0.02	26	0.018	2.308	0.034
WEB THICKNESS IN	WEBS PER INCH	CHANNEL WIDTH IN	WEB STRESS KSI	DH IN
0.008	20	0.042	13.125	0.072
0.012	20	0.038	7.917	0.066
0.015	20	0.035	5.833	0.061
0.02	20	0.030	3.750	0.053

The root cause of the distortion was identified and SolidWorks FEA analysis was utilized to refine the insert design to eliminate distortion. Specifically, the insert web sections and webs per inch were increased to lower stress on the web and joints. Besides adding strength to the core, the new insert impacts performance and cost. Table 10 lists the volume and weight performance parameters, M^3/UA and kg, for new insert configurations that have different channel cross-sections and channel separations. All of these cases are for the same heat transfer capability. For Case 1, the core strength is 30% higher than Case 2, but the volume and weight metrics are 7% and 44% higher. For Case 3, which is extra strong, the channel width control is reduced and the volume and weight metrics favorably reduced, at the expense of less uniformity in channel dimensions. Case 3 has 66% more core strength than Case 2, but volume and weight metrics are 39% and 32% lower than Case 2. Given the greater control on channel dimensions, Case 2 was chosen as best the insert configuration for the 50-kW unit design.

Table 10 – Revised Inserts Projected Performance

Insert Configuration	Web Thickness (in)	Channel Width (in)	Effectiveness (%)	M^3/UA	Kg/UA	Web Width/Channel Width
1 – Extra strong	.015	.023	94.8	.0030	18.98	.65
2 – Strong	.015	.03	94.4	.0028	13.22	.5
3 – Extra strong with higher channel width tolerances	.015	.018	94.7	.0017	9.00	.83

In addition to the core analysis, FEA was also used to confirm that the manifold design would have the needed strength with the new insert design. As part of this manifold assessment, capacities of HELC units were calculated where the outlet or inlet flow velocity is equal to the insert channel velocity. This equality gives a relative measure of the number of possible channel inserts before the manifold and outlet or inlet pressure drops become significant. Using this equality, the number of insert layers, overall height and capacity can be calculated for different channel widths. Table 11 presents the results for a single outlet or inlet per channel or two outlets and inlets per high or low pressure sides. As shown in Table 11, for the single outlet and inlet case, the number of layers, height and capacity increases with the channel width, with a capacity of 2.4 MWt estimated for a 58-inch core height and 16-inch channel width. For the 3,000 psi peak pressure, the manifold wall thickness needs to be 1.5-inches to keep the stress below the 16 ksi allowable limit. For the two outlets and inlets case, the number of layers, heights and capacities are reduced. However, the manifold wall thickness can also be reduced, as shown in Table 11. This will have some weight reduction benefit. From FEA results, it was concluded that both the insert and manifold designs had the needed strength for operating pressures of interest at 200 bar and a design temperature of 343 C.

Table 11 – Manifold Dimensions Relationship to HELC Core Height and Capacity

			ONE OUTLET AND INLET			
	OVERALL					
CHANNEL	CHANNEL	INLET	NUMBER	CORE	CAPACITY	MAINIFOLD
HEIGHT	WIDTH	DIAMETER	LAYERS	HEIGHT		WALL
IN	IN	IN		IN	KWT	IN
0.25	4	4	24	14.6	153.1	0.38
0.25	8	8	47	29.2	612.3	0.75
0.25	12	12	71	43.8	1377.7	1.13
0.25	16	16	94	58.4	2449.2	1.50
			TWO OUTLETS AND INLETS			
	OVERALL					
CHANNEL	WIDTH	INLET	NUMBER	CORE	CAPACITY	MAINIFOLD
HEIGHT	WIDTH	DIAMETER	LAYERS	HEIGHT		WALL
IN	IN	IN		IN	KWT	IN
0.25	4	2	12	7.3	76.5	0.19
0.25	8	4	24	14.6	306.2	0.38
0.25	12	6	35	21.9	688.8	0.56
0.25	16	8	47	29.2	1224.6	0.75

6.0 Cost Estimates

An important consideration in the commercialization of HELC is cost. Since large-scale HELC modules of 50 MW, as illustrated in Figure 8, have not been manufactured it is difficult to estimate production costs for full-scale modules at this time. However, costs for parts and services for 50 kW units fabricated under this effort can be utilized as a base for estimating costs for 500 KW and 5,000 kW capacity units that would be produced at limited production volumes. Given that the quotes were for limited production volumes these cost estimates will be conservative relative to large scale production costs.

Using the "Strong" insert configuration noted in Table 10, designs for 500 kW and 5,000 kW HELC heat exchangers were defined. Fabricator and material supplier cost quotes were then used to define the 500 kW prototype unit cost. These cost results were then extrapolated to the 5,000 kW unit case assuming that parts similar to those for the 500 kW unit can be used to construct the 5,000 kW unit. The cost for the 5,000 kW unit has significant uncertainty at this time, and more work will be required to better define the cost. Nevertheless, these estimates suggest the cost savings potential of HELC.

To estimate the cost of 500 kW and 5,000 kW units, the available heat transfer model was used to define heat exchanger component parameters. These components have significant similarities to the components illustrated in Figures 9, 10, 13, 14 and 16. Material and fabrication quotes for these components were then added together to define the cost for the 500 kW unit. Since these costs were for prototype-level units, the costs will be much higher than those for production units. To estimate production-level unit costs, the fabrication costs, including braze costs were adjusted to consider manpower application for cleaning, stacking, brazing and welding large-scale units. Results are given below.

The model uses REFPROP $ScCo_2$ properties, the J and f factor correlations of Liao and Zhao [8] and the geometrical factors for the final design inserts. These have three times the faying surface of the prior inserts to ensure an adequate safety margin even if an adjacent bond line fails. However, the extra faying surface increases solidity and weight of the HEX. The model gives the performance results for the 5,083 kW unit listed in Table 12. These performance results meet the required targets and are relatively consistent with earlier insert performance results listed in Tables 3, 4, 7 and 10. It should be noted that these predictions have not been confirmed by ScCO2 test data. However, the model results using water and oil fluids, shown in Figure 18, correspond with test results to within 10% at flow rates of interest. Therefore, $ScCO_2$ predicted results should be reasonable, if the small-diameter J and f correlations for $ScCO_2$ contained in reference 8 are valid.

Table 12 – HELC Predicted Performance

	HIGH PRESSURE	LOW PRESSURE
P(PSI)	3000	900
MDOT(LB/SEC)	132	132
Q(KW)	5083	
EFFECTIVENESS	95	
M3/UA	0.0019	
KG/UA	11.21	

HELC cost quotes from suppliers were used to develop HEX production costs. Table 13, provided on the following page, gives insert, frame separation plate and end plate costs for 500 kW and 5,083 kW HELCs. The quotes for the parts were based on quantities for five units. This only yielded a modest price reduction from suppliers. Under large unit volume production, quantities will be much larger and the price per part should be reduced. Therefore, results in Table 13 are conservative. In addition to the part costs, there are costs to clean and prepare parts, stack parts, braze the stack and weld on inlet and outlet connections. The quoted cost for these services is similar to the total part costs, as shown in Table 13. The total cost for the 500 kW HELC is then $41,306, which yields a cost of $82.61/kW. Taking these same part costs at a quantity of five, the 5,083 kW parts costs can be estimated by multiplying the 500 kW part count by 10 to estimate the 5,083 kW part count. Stacking up these identical 500 kW parts to achieve the 5,083 kW capacity would lead to a very tall stack. To improve manufacturability, it is assumed that the stack could have double the width of the 500 kW stack. This then reduces stack height by 50%, which makes it possible to fit the unit in the bonding furnace. For simplicity, this double-wide stack cost is considered to be the same as a single-wide configuration, except with the addition of two more end plates. Relative to the cleaning and stacking services costs, these could also be considered a factor of ten higher due to the higher part count. However, for brazing and welding the costs will not increase by a factor of 10. This then leads to the costs for the 5,083 kW unit included in Table 13. Summing the part and services costs then gives the total cost of $301,793, which yields a cost of $60.36/kW, which is a 27% lower cost per kW than the 500 kW case. For the calculated UA, the 5,083 kW case has a $1,349/UA. Relative to the recuperator cost metric of $1,500/UA noted in Full-Scale and Test Article design section, the HELC cost is 10% lower than the desired target. This shows the potential of the HELC approach. These costs are conservative. However, even considering the conservative cost estimate, HELC costs estimates in Table 4 are significantly below the estimated $92/kw for PCHE. For the 5,083 kW case the cost is reduced by 33.6%.

TABLE 13 – HELC Cost Estimates for 500 kW and 5,083kW Units

		HELC 500kW	HELC 5083kW			
		Units	Units	Cost/Unit	Quantity 5	Quantity 5
	Layers	23	230	$/Unit	HELC 500kW	HELC 5083kW
667-104-HP1	HP1 Inserts	46	460	$26.23	$1,206.58	$12,065.80
667-104-HP2	HP2 Inserts	46	460	$24.59	$1,131.14	$11,311.40
667-104-Blank	4.5" Inserts	230	540	$13.44	$3,091.20	$30,912.00
667-104-HP3	4.25" Inserts	23	270	$15.52	$356.96	$3,569.60
667-104-HP4	3.25" Inserts	23	270	$15.52	$356.96	$3,569.60
667-101	HP frame	23	230	$182.20	$4,190.54	$41,905.38
667-102	LP frame	23	230	$182.20	$4,190.54	$41,905.38
667-103	Plate 42	46	540	$54.44	$2,504.34	$25,043.38
667-122	Top Endplate	1	2	$2,160.00	$2,160.00	$4,320.00
667-123	Bottom Endplate	1	2	$1,940.00	$1,940.00	$3,880.00
					$21,128.25	$178,482.54
	Brazing and Welding Operations				$20,178.00	$123,310.00
		Cleaning				
		stacking				
		braze run				
		Welding gussets and fittings				
					$41,306.25	$301,792.54
					$82.61	$60.36

7.0 Conclusions

As an alternative to expensive Printed Circuit Heat Exchangers (PCHE) used in the gas and oil industries, a purpose-built high pressure and effectiveness recuperator was identified to provide the reliability, compactness, performance and pressure capability of current recuperators, but at a reduced cost. Using recuperator specifications defined by Echogen, the heat exchanger process design was prepared using a proprietary heat transfer and pressure drop model. Test results proved a model accuracy of 10% at flow rates of interest. Model results covered the impact of heat exchanger channel height and length, hydraulic diameter, open area and number of channels on heat transfer and pressure drop performance. The calculated HELC volume and weight metrics of .0024 m^3/UA and 10.2 kg/UA were found to be 4% and 77.3% below recuperator desired target metrics defined by Echogen, showing the potential of the concept. Given this potential, the process parameters were then used to prepare mechanical designs for a sub-scale test article that would produce the needed performance and demonstrate the integrity and manufacturability of the design. In addition to the 50 kWt test article design, 500 kW and 5,000 kWt modules were designed that could be used as a base unit to create an array of 50,000 kW units for full-scale power plant operations. The 50 KWt test article was fabricated using 316 stainless steel frames, plates and inserts that were bonded in a vacuum furnace using a nickel-based braze alloy. Following test article buildup, the HELC unit was tested using oil and water to validate the proprietary heat transfer and pressure drop model. This model was then used to predict HELC performance on supercritical CO_2 using small-diameter tube heat transfer and pressure drop correlations. These results supported the volume and weight advantages of HELC over PCHE recuperators. Following heat exchanger performance tests, the HELC was hydrostatically tested to demonstrate the integrity of the design. The first test unit developed a leak at a pressure below the operating pressure. Investigation suggested that the leak was a result of insufficient braze amount and a lower than optimal temperature profile. After adjusting the braze amount and temperature profile a second test unit was built. Pressure tests of the second unit at up to 4,000 psi differential pressure showed no evidence of leaks, but it was found that the channel inserts were distorted. Investigation indicated that stress concentrations were excessive. To alleviate stress concentrations, the design of the inserts and manifolds were updated and the design and test article costs were used to estimate the costs of 500 kW and 5,083 kW HELC units. The 5,083 kW unit costs were $1,349/UA, which is 10% below the Echogen recuperator cost metric of $1,500/UA. In addition, the estimated cost of $60.09/kW is 33.6% below the $92/kW for PCHE recuperators.

Based on the analysis and performance test results, the HELC design has the potential to reduce volume, weight and cost metrics versus PCHE designs. The final updated design is expected to improve the pressure capability of HELC. More development and test work is required to confirm this capability.

References

1. Dostal, V., Driscoll, M. and Hejzlar, P., "A Supercritical Carbon Dioxide Cycle for Next Generation Nuclear Reactors", MIT-ANP-TR-100, March 2004
2. Carlson, M. D., Schalansky, C., Kruizenga, A. K., Fleming, D.F., "Sandia Progress on Advanced Heat Exchangers for SCO2 Brayton Cycles", The 4th International Symposium – Supercritical CO2 Power Cycles, September 9-10, 2014, Pittsburgh, Pennsylvania
3. Southall, D., Le Pierres, R., Dewson, S. J., "Design Considerations for Compact Heat Exchangers", Proceedings of ICAPP '08, Anaheim, CA., June 8-12, 2008, Paper 8009
4. Matson, D., et al, "Fabrication of Microchannel Chemical Reactors Using a Metal Lamination Process", Pacific Northwest National Laboratory, Richland, WA.
5. Echogen
6. Kays, W.M., London, A.L., "Compact Heat Exchangers", Third Edition, Krieger Publishing Company, Malabar, FL., 1984
7. Liao, S.M., Zhao, T.S., "A Numerical Investigation of Laminar Convection of Supercritical Carbon Dioxide in Vertical Mini/Micro Tubes", Progress in Computational Fluid Dynamics, Vol. 2, Nos. 2/3/4, 2002
8. Liao, S.M., Zhao, T.S., "Measurements of Heat Transfer Coefficients from Supercritical Carbon Dioxide Flowing in Horizontal Mini/Micro Channels", Journal of Heat Transfer, June, 2002, Vol. 124/ 413
9. www.solidworks.com
10. www.asme.org
11. www.heatric.com
12. www.wallcolmonoy.com